Electroweak Sudakov effects in W, Z and γ production at large transverse momentum

Thomas Becher and Xavier Garcia i Tormo

Albert Einstein Center for Fundamental Physics, Institut für Theoretische Physik,
Universität Bern, Sidlerstrasse 5, CH-3012 Bern, Switzerland

We study electroweak Sudakov effects in single W, Z and γ production at large transverse momentum using soft collinear effective theory. We present a factorized form of the cross section near the partonic threshold with both QCD and electroweak effects included and compute the electroweak corrections arising at different scales. We analyze their size relative to the QCD corrections as well as the impact of strong-electroweak mixing terms. Numerical results for the vector-boson cross sections at the Large Hadron Collider are presented.

I. INTRODUCTION

The production of a single electroweak boson is one of the basic hard-scattering processes that one can measure at hadron colliders. Much theoretical effort has been put over the years into precisely predicting the cross section of the W, Z, and γ production processes. There is ongoing work to obtain the second-order corrections in the strong coupling α_s to the transverse momentum spectrum, a quantity for which the next-to-leading order results are known for a long time [1–3] and have been implemented in numerical integration programs [4–8]. One way to improve the fixed-order results is to include resummation of higher-order terms that are enhanced in certain kinematical limits. Here, we focus on the region of large transverse momentum p_T and compute the cross section near the partonic threshold. In this region, two types of Sudakov-enhanced terms arise, whose combined resummation is the subject of the present paper. First of all, the electroweak corrections are enhanced by double logarithms of the vector-boson masses M_W and M_Z over p_T. Secondly, near threshold, the invariant mass of the hadronic jet which recoils against the electroweak boson is small and the perturbative corrections are enhanced by logarithms of the jet mass M_X over p_T. One can expand around the threshold limit and resum the enhanced terms. For the electroweak-boson spectrum, threshold resummation was first achieved at next-to-leading logarithmic accuracy in [9]. Except in the unrealistic case where the p_T value is close to the maximum kinematically allowed value, the cross section also receives contributions away from the threshold region. However, the partonic threshold contributions often amount to the bulk of the hadronic cross section. This is due to the rapid falloff of the parton distribution functions (PDFs) $f(x)$ at large x, which dynamically enhances the threshold region (see Ref. [10] and references therein).

In the partonic threshold limit, the real radiation simplifies considerably because of the restricted phase space. The hadronic final state consists of the electroweak vector boson recoiling against a single low-mass jet, and all additional hadronic radiation must be either soft, or collinear to the jet or the incoming hadrons. This kinematical situation is amenable to an effective theory treatment using soft collinear effective theory (SCET) [11–13]. Within the SCET framework, threshold resummation of quantum chromodynamics (QCD) corrections for W, Z and γ production at large p_T has been achieved at next-to-next-to-leading logarithmic (N^{2}LL) accuracy [14–16]. Some results with N^{2}LL accuracy were also presented in Ref. [17], using the traditional diagrammatic approach to resummation. Essentially all the ingredients required to achieve next-to-next-to-next-to-leading logarithmic (N^{3}LL) accuracy in the SCET framework are by now known [18–24] and a complete analysis of resummation at N^{3}LL accuracy will be the subject of a future publication.

At the energies and luminosities that the Large Hadron Collider (LHC) can reach, also virtual corrections due to electroweak-boson exchanges can become quite significant. Since we are considering single electroweak-boson production, without additional radiation of soft or collinear W or Z bosons, the cross section will contain logarithms of the form $\ln (p_T^2/M_V^2)$, where M_V is the W- or Z-boson mass. This was recognized long ago, and the electroweak one-loop corrections and two-loop logarithmically enhanced terms have been computed for these processes [25–30]. The outcome of these analyses is that electroweak corrections can be as large as 20% for $p_T \sim 1$ TeV at the LHC, clearly indicating that electroweak Sudakov effects have to be included if one wants to have a precise prediction for the spectrum in the region $p_T \gg M_V$. Let us note that these logarithms would partly cancel if one considered real W and Z emission, in addition to virtual electroweak-boson exchanges, but the cancellation would not be complete, since the initial states carry non-Abelian charge [31]. Recently, this was explicitly verified for the $Z + 1$ jet production process at the double-logarithmic level [32]. In this paper we elaborate on the inclusion of electroweak effects in the cross sections using SCET.

A derivation of the factorization formula for single electroweak-boson production within SCET has been

given in Ref. [14]. The factorization formula will be made more explicit in the following sections, but schematically we have that the partonic cross section $\hat{\sigma}$ is given in a factorized form as

$$d\hat{\sigma} \sim \hat{\sigma}^B H \times J_V \otimes J \otimes S, \qquad (1)$$

where $\hat{\sigma}^B$ is the Born cross section, H the hard function, and J and S the jet and soft functions, which encode collinear and soft radiation, respectively. The symbol $\otimes$ denotes a convolution. Since we will deal with electroweak corrections, in addition to strong-interaction effects, we have included a jet function J_V for the electroweak boson $V = W, Z, \gamma$ in the factorization formula. The formalism to incorporate electroweak corrections in the SCET framework was developed in a series of papers by Chiu *et al.* [33–37]. In those papers, resummation of electroweak Sudakov corrections to the hard function H was studied in detail, and explicit expressions for several different hard-scattering processes were given. The strategy to incorporate electroweak corrections consists of four steps [36]: (i) a matching from the full Standard Model (SM) to SCET at a high scale $\mu_h \sim p_T$. (ii) Running from μ_h to a low scale $\mu_l \sim M_V$. (iii) Matching at the scale μ_l, from a version of SCET that contains dynamical Z and W bosons to a version of SCET where those massive gauge bosons, together with the top quark and the Higgs boson, are integrated out. Following Ref. [36] we denote the theory below μ_l as SCET_γ, and the theory above μ_l as $\mathrm{SCET}_{\mathrm{EW}}$. The final step (iv) consists of the running from μ_l to the factorization scale μ_f. Steps (i) and (ii) are independent of the masses of the gauge bosons, and of the pattern of electroweak symmetry breaking, and can be performed in the unbroken theory, with massless particles. The jet and soft functions are then defined in SCET_γ and only contain photon, gluon and light-fermion radiation. We denote by μ_j and μ_s the scales where the jet and soft functions are defined, respectively. This whole setup is illustrated in Fig. 1. In this paper, we study in detail the importance of electroweak corrections to the different ingredients of the factorization formula and discuss the best way to set the different factorization scales when both QCD and electroweak corrections are included.

Before going on, a comment regarding the definition of the observable we are considering is in order, which is no longer unambiguous once electroweak corrections are included. In particular, we need to clarify what we mean by a jet. In the full SM, when one computes electroweak corrections to $V + \mathrm{jet}$ one will encounter real radiation diagrams where there is a photon and a gluon or quark in the final state. The p_T of the electroweak boson V can be balanced by both the recoiling parton and the photon. As a consequence, the singularities of the real-emission diagrams cancel in part with virtual electroweak corrections to $V + \mathrm{jet}$ but also in part with QCD corrections to the $V + \gamma$ process. One should therefore either put some cut
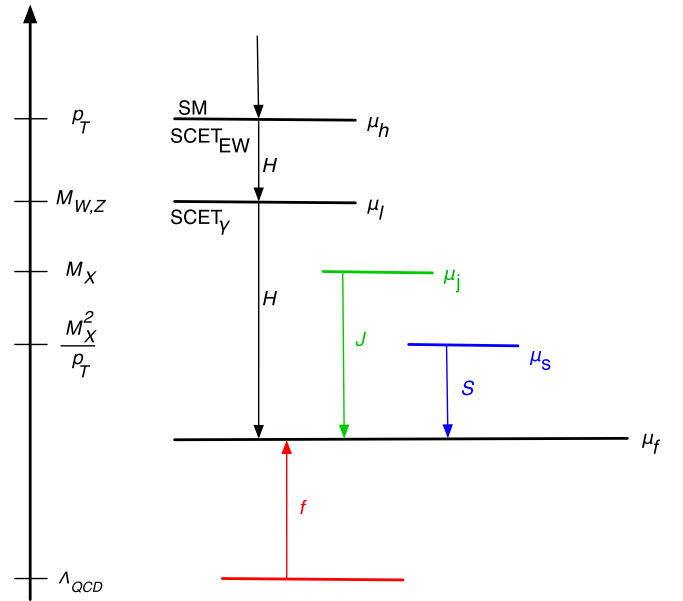

FIG. 1 (color online). Effective theory setup. H, J, S, and f denote the hard, jet, and soft functions, and the PDFs, respectively; Λ_{QCD} is the QCD scale.

which excludes configurations where the p_T of the V is compensated by a hard photon, or consider a more inclusive observable and include also the $V + \gamma$ process with its QCD corrections. Either option amounts to a well-defined observable, and both of them were discussed in the literature [29,30]. In addition, Refs. [38,39] present electroweak corrections including the leptonic W and Z decay. Comparisons between the different results seem to indicate that the the size of the corrections is very similar in the two cases [30]. Here, we consider single-boson production near threshold, where the factorization formula Eq. (1) for the partonic cross section is valid. Since we consider inclusive V production in the threshold limit, the real radiation is encoded in the soft and jet functions, with no phase space for additional hard radiation. At leading order in the power counting in the effective theory one will have operators which, in addition to the vector boson V, involve (i) a collinear quark or gluon field, or (ii) a collinear photon in the final state. Obviously the first operators give $V + \mathrm{jet}$, while the second ones give $V + \gamma$ at Born level. The different operators do not mix, and we can consider them separately. We will not include operator (ii) in the following. The quark (and gluon) jet functions contain collinear photons, but soft quark radiation is power suppressed in the threshold limit and a quark jet function will not lead to contributions where a photon carries all the energy. Therefore by considering the threshold limit, and writing down the factorized formula in the effective theory, we avoid the need to introduce an explicit cut to exclude a hard photon. The cut would affect power-suppressed terms, whose size will govern its importance.

The rest of the paper is organized as follows. In Sec. II, we first we describe the kinematics of the process and

specify the power counting that we use. We then give general expressions for the anomalous dimensions and the matching corrections and discuss how the result for specific channels can be obtained. Section III contains the results and plots for Z and γ production, while Sec. IV contains the ones for W bosons. In Sec. V we discuss the size of the electroweak corrections, compare with results from the literature and conclude. The Appendix collects the beta functions that enter in our results.

II. PRELIMINARIES

A. Kinematics and power counting

There are two partonic channels that are relevant for single electroweak-boson production at leading order: the Compton channel $qg \rightarrow qV$, and the annihilation channel $q\bar{q} \rightarrow gV$, plus permutations of the initial-state partons or interchange of q and $\bar{q}$. At next-to-next-to-leading order also the channel $gg \rightarrow gV$ contributes, but it is only relevant

for N^{3}LL accuracy, and we don't need to consider it here. The partonic Mandelstam variables for $ab \rightarrow cV$ are given by $\hat{s} = (p_a + p_b)^2$, $\hat{t} = (p_a - p_V)^2$, and $\hat{u} = (p_b - p_V)^2$. Throughout the paper, a hat denotes a partonic quantity.

We now define a counting to be able to specify which terms in the amplitude will be kept in our results. Defining a as the counting parameter, we use

$$\alpha_s \sim a; \qquad L := \log \frac{p_T^2}{M_Z^2} \sim \frac{1}{a}; \qquad \alpha_i \sim a^2, \quad (2)$$

where α_s is the strong coupling and α_i is the $SU(2)_L$ or $U(1)_Y$ coupling (α_2 or α_1, respectively; or the electromagnetic coupling $\alpha_{\rm em}$, if we are in SCET$_\gamma$). As was done in Ref. [35], we find it convenient to present a table with the different terms entering in the amplitude. If we denote the amplitude by $\mathcal{M}$, we have, schematically, that the log of the amplitude will contain the following terms:

$$\log \mathcal{M} \sim \begin{pmatrix} \alpha_s L^2 + \alpha_i L^2 & \alpha_s L + \alpha_i L & \alpha_s + \alpha_i \\ \sim \frac{1}{a} + 1 & \sim 1 + a & \sim a + a^2 \\ \alpha_s^2 L^3 + \alpha_i^2 L^3 & \alpha_s^2 L^2 + \alpha_i^2 L^2 & \alpha_s^2 L + \alpha_s \alpha_i L + \alpha_i^2 L & \alpha_s^2 + \alpha_s \alpha_i + \alpha_i^2 \\ \sim \frac{1}{a} + a & \sim 1 + a^2 & \sim a + a^2 + a^3 & \sim a^2 + a^3 + a^4 \\ \alpha_s^3 L^4 + \alpha_i^3 L^4 & \alpha_s^3 L^3 + \alpha_s^2 \alpha_i L^3 + \alpha_s \alpha_i^2 L^3 + \alpha_i^3 L^3 & \vdots & \ddots \\ \sim \frac{1}{a} + a^2 & \sim 1 + a + a^2 + a^3 \\ \vdots & \vdots \end{pmatrix}, \quad (3)$$

where it is understood that the amplitude is normalized such that tree level corresponds to $\mathcal{M} = 1$. To obtain the above table, one needs to take into account that the β functions in the SM contain terms involving couplings from different gauge groups starting at two loops, and that the cusp anomalous dimension contains terms that mix the couplings starting at four loops. For the pure-QCD terms, N^{k-1}LL accuracy corresponds to keeping all the terms in the first k columns of the table of Eq. (3). Pure-QCD terms were considered at N^{2}LL accuracy in Refs. [14–16]; here we will also consider the rest of the terms, which involve at least one α_i.

B. Renormalization-group evolution of the hard function

In the effective theory, the resummation is performed by solving renormalization-group (RG) equations for the hard, jet and soft functions and evolving them to a common scale. To set the stage for the explicit expressions given in the next sections, we now give general expressions for the necessary hard anomalous dimensions and the solution of the associated RG equations. The hard functions are

given by renormalized on-shell amplitudes. For massless particles and at the one-loop level, their evolution is governed by the anomalous dimension [40,41]

$$\mathbf{\Gamma}(\{\underline{p}\}, \mu) = \sum_{i<j} \frac{\alpha}{4\pi} \mathbf{T}_i \cdot \mathbf{T}_j \Gamma_0 \ln \frac{\mu^2}{-s_{ij}} + \sum_i \frac{\alpha}{4\pi} \gamma_0^i, \quad (4)$$

where $\{\underline{p}\}$ represents the set of momentum vectors of the external particles, $s_{ij} := 2\sigma_{ij} p_i \cdot p_j + i0$, and the sign factor $\sigma_{ij} = +1$ if the momenta p_i and p_j are both incoming or outgoing, and $\sigma_{ij} = -1$ otherwise. The product $\mathbf{T}_i \cdot \mathbf{T}_j = \sum_a T_i^a T_j^a$, where T_i^a are the gauge-theory generators in the representation relevant for particle i (see e.g. Ref. [41] for more details). This expression is valid for a general unbroken gauge theory with coupling constant α. The one-loop cusp anomalous dimension is $\Gamma_0 = 4$ and the collinear anomalous dimension γ_0^i depends on the representation and the spin of the particle. For a fermion, one has $\gamma_0^q = -3C_F$, while it takes the value $\gamma_0^g = -\beta_0$ for a gauge boson, where it is understood that one uses the Casimir C_F and first beta function coefficient β_0 that are appropriate for the corresponding gauge group.

Because we count $\alpha_1 \sim \alpha_2 \sim a^2$, the one-loop expression for the anomalous dimension is sufficient for the electroweak corrections at order a. However, we note that there are strong all-order constraints on the anomalous dimension [40–45], which imply in our case that the structure of the anomalous dimension remains the same up to, at least, three-loop order.

The relevant theory for the hard functions at $\mu \sim p_T \gg M_V$ is the SM in the unbroken phase, and one has to replace

$$\frac{\alpha}{4\pi}\boldsymbol{T}_i \cdot \boldsymbol{T}_j \to \frac{\alpha_1}{4\pi}Y_i \cdot Y_j + \frac{\alpha_2}{4\pi}\boldsymbol{t}_i \cdot \boldsymbol{t}_j + \frac{\alpha_s}{4\pi}\boldsymbol{T}_i \cdot \boldsymbol{T}_j \quad (5)$$

in the above expression, Eq. (4), for the anomalous dimension. Here Y_i is the hypercharge of particle i, and $\boldsymbol{t}_i$ and $\boldsymbol{T}_i$ the generators associated with $SU(2)_L$ and $SU(3)_C$, in the appropriate representation for particle i. The relevant theory for the running below μ_l is QCD + QED and the anomalous dimensions are obtained by substituting

$$\frac{\alpha}{4\pi}\boldsymbol{T}_i \cdot \boldsymbol{T}_j \to \frac{\alpha_{\mathrm{em}}}{4\pi}Q_i \cdot Q_j + \frac{\alpha_s}{4\pi}\boldsymbol{T}_i \cdot \boldsymbol{T}_j \quad (6)$$

in the general expression, where Q_i is the electric charge of particle i.

In our case, the hard amplitudes are $q\bar{q} \to gV$ and crossings thereof. They involve only three charged particles under any of the gauge groups. In the three-particle case, charge conservation $\sum_i \boldsymbol{T}_i = 0$ can be used to rewrite the color-dipole terms in the form

$$2\sum_{i<j}\boldsymbol{T}_i \cdot \boldsymbol{T}_j \ln\frac{\mu^2}{-s_{ij}} = -(C_1 + C_2 - C_3)\ln\frac{\mu^2}{-s_{12}}$$
$$- (C_1 + C_3 - C_2)\ln\frac{\mu^2}{-s_{13}}$$
$$- (C_2 + C_3 - C_1)\ln\frac{\mu^2}{-s_{23}}, \quad (7)$$

where $C_i = \boldsymbol{T}_i \cdot \boldsymbol{T}_i$ is the quadratic Casimir operator associated with leg i. This makes it clear that the anomalous dimensions for vector-boson production are diagonal in gauge-group space.

Below, we will write the RG equation for the hard function for production of a vector boson V in the partonic channel $ab \to cV$ in the form

$$\frac{d}{d\ln\mu}H_{ab,V}(\hat{s}, \hat{t}, \mu) = \left[\Gamma^{(V)}\ln\frac{\hat{s}}{\mu^2} + \gamma_{ab}^{(V)}\right]H_{ab,V}(\hat{s}, \hat{t}, \mu),$$
$$(8)$$

where we suppress the dependence of the noncusp anomalous dimension $\gamma_{ab}^{(V)}$ on $\hat{s}$ and $\hat{t}$. We write the solution to this equation in terms of an evolution factor times the hard function at a high scale ν:

$$H_{ab,V}(\hat{s}, \hat{t}, \mu) = \mathcal{U}_{ab}^{(V)}(\nu, \mu)H_{ab,V}(\hat{s}, \hat{t}, \nu). \quad (9)$$

At the order we are working, we do not need to consider electroweak corrections to the matching, and the functions $H_{ab,V}(\hat{s}, \hat{t}, \mu_h)$ are then given by the corresponding QCD results. We thus do not need to distinguish the $U(1)_Y$ hard function $H_{ab,B}(\hat{s}, \hat{t}, \mu_h)$ from the $SU(2)_L$ hard function $H_{ab,W^3}(\hat{s}, \hat{t}, \mu_h)$ and will denote the common QCD hard function for Z-boson production simply by $H_{ab,Z}(\hat{s}, \hat{t}, M_Z, \mu_h)$. We furthermore keep the power-suppressed M_Z dependence both in $H_{q\bar{q},Z}(\hat{s}, \hat{t}, M_Z, \mu_h)$ and in the Born-level cross sections.

The pure-QCD hard functions and their evolution were given in [14,16]. The contribution of the electroweak gauge coupling α_i to the evolution factor has the following form:

$$\ln\mathcal{U}_{ab}^{(V)}(\nu, \mu)\big|_{\alpha_i} = 2S^{(V)}(\nu, \mu) - A_{ab}^{(V)}(\nu, \mu)$$
$$- \ln\frac{\hat{s}}{\nu^2}A_\Gamma^{(V)}(\nu, \mu) + 2S_{\alpha_s\alpha_i}(\nu, \mu), \quad (10)$$

where the functions $S^{(V)}(\nu, \mu)$ and $A_{ab}^{(V)}(\nu, \mu)$ are [14,46]

$$S^{(V)}(\nu, \mu) = -\int_{\alpha_i(\nu)}^{\alpha_i(\mu)}d\alpha\frac{\Gamma^{(V)}(\alpha)}{\beta(\alpha)}\int_{\alpha_i(\nu)}^{\alpha}\frac{d\alpha'}{\beta(\alpha')};$$
$$A_{ab}^{(V)}(\nu, \mu) = -\int_{\alpha_i(\nu)}^{\alpha_i(\mu)}d\alpha\frac{\gamma_{ab}^{(V)}(\alpha)}{\beta(\alpha)}. \quad (11)$$

The function $A_\Gamma^{(V)}(\nu, \mu)$ is obtained by replacing $\gamma_{ab}^{(V)}$ with $\Gamma^{(V)}$ in $A_{ab}^{(V)}(\nu, \mu)$. It is understood that the appropriate anomalous dimension and beta function for each coupling is used in Eq. (11). The explicit expressions for the beta function coefficients appearing throughout the paper are collected in the Appendix. In addition to the contributions from the individual gauge groups, we also need to take into account mixing terms at the order we are working. These are encoded in the last term in Eq. (10). The mixing contribution is $S_{\alpha_s\alpha_{1,2}}$ when $V = W^{1,2,3}$ or B, and $S_{\alpha_s\alpha_{\mathrm{em}}}$ when $V = Z$, $W^\pm$, or γ, for the hard running below the scale μ_l. It is given by the function $S(\nu, \mu)$ for the strong coupling keeping only the terms of order a that contain one α_i, which come from the expansion of the beta function for α_s in the denominators of Eq. (11). These corrections correspond to the terms with one α_i and an arbitrary number of α_s in the second column of Eq. (3), all of which are of order a. For the second stage of hard running, below the scale μ_l, the logarithm $\ln\hat{s}/\mu_l^2$ arising in Eq. (10) is large because $\mu_l^2 \ll \hat{s}$. In this case, we also need to include a mixing term $A_{\alpha_s\alpha_{\mathrm{em}}}$ arising in the function $A_\Gamma^{(V)}$.

C. Collinear factorization anomaly

For massive Sudakov problems, the individual collinear and soft diagrams are not well defined and need additional regularization beyond the standard dimensional regularization. This can be done with an analytic regulator [47]. The additional regulator can be removed once the

contributions from the individual collinear regions are combined, but as a result a large logarithm arises in the matching of SCET$_{EW}$ to SCET$_\gamma$ [33]. The presence of large logarithms in the matching is problematic since such logarithms are not generated by RG evolution but need to be resummed. This collinear anomaly also arises in many other observables, in particular in transverse-momentum dependent quantities [48]. It was shown in [34] that the additional logarithm exponentiate. The exponentiation is derived from the requirement that the regulator dependence must cancel among the different collinear and soft pieces [34,48], or alternatively, from solving an evolution equation in the associated regulator scale [49].

While the standard electroweak matching corrections are beyond our accuracy, the logarithmically enhanced pieces due to the collinear anomaly need to be included. One-loop collinear functions for the Standard Model were given in [37]. The logarithmically enhanced piece has the general form

$$D_C^i = \frac{\alpha}{4\pi}\frac{\Gamma_0}{4}\boldsymbol{T}_i \cdot \boldsymbol{T}_i \ln\frac{M^2}{\mu^2}\ln\frac{\hat{s}}{\mu^2}, \qquad (12)$$

where α stands for the coupling of the broken gauge group whose boson has a mass M. The full one-loop expression involves a sum over pairs like Eq. (4), but since we only need the leading logarithmic contribution, we have replaced $s_{ij} \rightarrow -\hat{s}$ and have used charge conservation $\sum_i \boldsymbol{T}_i = 0$ to write it in the above form. These collinear functions need to be computed in the broken phase and to obtain them, one replaces [37]

$$\alpha\boldsymbol{T}_i \cdot \boldsymbol{T}_i \rightarrow \alpha_W(\boldsymbol{t}_i \cdot \boldsymbol{t}_i - (t_i^3)^2) + \alpha_Z(t_i^Z)^2, \qquad (13)$$

where $t^Z = t^3 - s_W^2 Q$, $\alpha_W = \alpha_2$, and $\alpha_Z = \alpha_1/s_W^2 = \alpha_2/c_W^2 = \alpha_{em}/(c_W^2 s_W^2)$, with $c_W := \cos\theta_W$, $s_W := \sin\theta_W$, and θ_W the weak-mixing angle. To obtain the eigenvalues of the Casimir operators acting on the W-boson fields, we need to work with the generators in the adjoint representation. We find

$$(\boldsymbol{t}\cdot\boldsymbol{t} - (t^3)^2)|W^\pm\rangle = |W^\pm\rangle,$$
$$(\boldsymbol{t}\cdot\boldsymbol{t} - (t^3)^2)|W^3\rangle = 2|W^3\rangle,$$
$$(t^Z)^2|W^\pm\rangle = c_W^4|W^\pm\rangle,$$
$$(t^Z)^2|W^3\rangle = 0.$$

We will use the notation

$$D_{q\bar{q}}^{(W^3\rightarrow Z)}(\mu) = D_C^q + D_C^{\bar{q}} + D_C^{W^3} \qquad (14)$$

for the collinear function for Z-boson production arising from the operator with field content $q\bar{q}W^3$ (and analogous notations for the rest of the collinear functions). As we stated above, this contribution exponentiates, so the relevant factor in the cross section is

$$\mathcal{D}_{q\bar{q}}^{(W^3\rightarrow Z)}(\mu) = e^{D_{q\bar{q}}^{(W^3\rightarrow Z)}(\mu)}. \qquad (15)$$

III. RESULTS FOR Z AND γ PRODUCTION

We now give the results for Z production and will afterwards discuss how they must be modified to also obtain the cross section for γ production. The hadronic cross section for the Z-boson case is given by

$$\frac{d\sigma_Z}{dp_T dy} = 2p_T\sum_{ab}\int dx_1 dx_2 f_a(x_1)f_b(x_2)\left[\hat{s}\frac{d\hat{\sigma}_{ab,Z}}{d\hat{s}d\hat{t}}\right], \qquad (16)$$

where $f_a(x)$ is the PDF for parton a. The sum runs over a, $b = q$, $\bar{q}$, g, and y is the Z's rapidity. The factorized form for the partonic cross section for the channel $ab \rightarrow cZ$ is [14,15]

$$\hat{s}\frac{d\hat{\sigma}_{ab,Z}}{d\hat{s}d\hat{t}} = \hat{\sigma}_{ab,Z}^B H_{ab,Z}(\hat{s},\hat{t},M_Z,\mu)$$
$$\times \int dk J_c(M_X^2 - 2E_J k, \mu)S_{ab,Z}(k,\mu), \qquad (17)$$

where $M_X^2 = (p_a + p_b - p_Z)^2$, and E_J is the energy of the jet. At Born level $J_c(p^2,\mu)$ and $S_{ab,Z}(k,\mu)$ reduce to delta functions of their first arguments, and the hard function $H_{ab,Z}$ is equal to 1. The Born-level cross sections are given by

$$\hat{\sigma}_{q\bar{q},Z}^B = \frac{\pi\alpha_{em}\alpha_s}{\hat{s}}\frac{2C_F}{N_c}(I^Z)^2\left(\frac{\hat{t}^2 + \hat{u}^2 + 2M_Z^2\hat{s}}{\hat{t}\hat{u}}\right);$$
$$\hat{\sigma}_{qg,Z}^B = -\frac{\pi\alpha_{em}\alpha_s}{\hat{s}}\frac{1}{N_c}(I^Z)^2\left(\frac{\hat{t}^2 + \hat{s}^2 + 2M_Z^2\hat{u}}{\hat{t}\hat{s}}\right), \qquad (18)$$

with $C_F = (N_c^2 - 1)/(2N_c)$, N_c the number of colors, and $I^Z := (\frac{c_W}{s_W}t^3 - \frac{s_W}{c_W}Y)$, with t^3 the weak isospin and Y the hypercharge (the electric charge Q is given by $Q = t^3 + Y$). Note that we keep the M_Z terms in the Born-level cross section, and in kinematical factors.

The Z boson in the low-energy broken theory can come from the $U(1)_Y$ gauge boson B or the $SU(2)_L$ gauge boson W^3 in the unbroken theory. We therefore need to consider the amplitudes $ab \rightarrow cW^3$ and $ab \rightarrow cB$ in the high-energy unbroken theory, and combine them according to $Z = c_W W^3 - s_W B$, which can be thought of as part of the tree-level matching condition at μ_l. For the pure-QCD terms, the log resummation is the same for the B and W^3 terms, and therefore the amplitude is still proportional to I^Z after resummation, but when we include electroweak corrections the B and W^3 terms receive different contributions and the resummed amplitude is no longer proportional to I^Z. The external Z, and the external W in the next section, are treated with a boosted version of a heavy quark effective theory (HQET) field in SCET$_\gamma$ [36,50] (we use the

standard name HQET, despite the fact that the heavy particle is not a quark in our case). Since the Z is neutral, its jet function J_Z is trivial (i.e. exactly a δ function), and it does not appear explicitly in the factorization formula in Eq. (17). That is, we have already integrated over the associated convolution variable that would appear in Eq. (1).

A. Cross section in SCET

In this section we present the results for the different ingredients that enter in the factorized cross section formula in SCET, Eqs. (16) and (17). The hard function (times Born-level cross section) for the annihilation channel is given by

$$
\hat{\sigma}^B_{q\bar{q},Z} H_{q\bar{q},Z}(\hat{s}, \hat{t}, M_Z, \mu_f) = \frac{\pi \alpha_s(\mu_h)}{\hat{s}} \frac{2 C_F}{N_c} \left(\frac{\hat{t}^2 + \hat{u}^2 + 2 M_Z^2 \hat{s}}{\hat{t}\,\hat{u}} \right) |\mathcal{U}^{(Z)}_{q\bar{q}}(\mu_l, \mu_f)|^2 |c_W \sqrt{\alpha_2(\mu_h)} t^3 \mathcal{D}^{(W^3 \to Z)}_{q\bar{q}}(\mu_l) \mathcal{U}^{(W^3)}_{q\bar{q}}(\mu_h, \mu_l)
$$

$$
- s_W \sqrt{\alpha_1(\mu_h)} Y \mathcal{D}^{(B \to Z)}_{q\bar{q}}(\mu_l) \mathcal{U}^{(B)}_{q\bar{q}}(\mu_h, \mu_l)|^2 H_{q\bar{q},Z}(\hat{s}, \hat{t}, M_Z, \mu_h). \tag{19}
$$

In Eq. (19), the $\mathcal{U}^{(V)}_{q\bar{q}}(\mu_h, \mu_l)$ factors encode the running from μ_h to μ_l in SCET$_{EW}$, and $\mathcal{U}^{(Z)}_{q\bar{q}}(\mu_l, \mu_f)$ the running from μ_l to μ_f in SCET$_\gamma$. The general structure of the anomalous dimensions was given in Sec. II B, we present in the following the expressions needed to account for the terms up to order a in Eq. (3). The explicit results for the electroweak part of the anomalous dimensions we need are

$$
\Gamma^{(W^3)} = \frac{\alpha_1}{4\pi} Y^2 \Gamma_0 + \frac{\alpha_2}{4\pi} \frac{7}{4} \Gamma_0, \qquad \gamma^{(W^3)}_{q\bar{q}} = \frac{\alpha_1}{4\pi} Y^2 (-6 - i\pi\Gamma_0) + \frac{\alpha_2}{4\pi} \frac{1}{4} \left(-18 - 4\beta^{\alpha_2}_0 + i\pi\Gamma_0 - 4\Gamma_0 \log\frac{\hat{s}^2}{\hat{t}\,\hat{u}} \right),
$$

$$
\Gamma^{(B)} = \frac{\alpha_1}{4\pi} Y^2 \Gamma_0 + \delta_{\lambda L} \frac{\alpha_2}{4\pi} \frac{3}{4} \Gamma_0, \qquad \gamma^{(B)}_{q\bar{q}} = \frac{\alpha_1}{4\pi} [Y^2(-6 - i\pi\Gamma_0) - \beta^{\alpha_1}_0] + \delta_{\lambda L} \frac{\alpha_2}{4\pi} \frac{3}{4}(-6 - i\pi\Gamma_0), \tag{20}
$$

$$
\Gamma^{(Z)} = \frac{\alpha_{\text{em}}}{4\pi} Q^2 \Gamma_0, \qquad \gamma^{(Z)}_{q\bar{q}} = \frac{\alpha_{\text{em}}}{4\pi} Q^2 (-6 - i\pi\Gamma_0),
$$

where $\lambda = L, R$ indicates if the quark is left or right handed.

The factors $\mathcal{D}^{(V \to B)}_{q\bar{q}}(\mu_l)$ encode the matching from SCET$_{EW}$ to SCET$_\gamma$ at μ_l. Using the results of Sec. II C, the relevant functions are obtained as

$$
D^{(W^3 \to Z)}_{q\bar{q}}(\mu) = \frac{1}{4\pi} 2 \log\frac{\hat{s}}{\mu^2} \left[\alpha_{\text{em}}(I^Z)^2 \log\frac{M_Z^2}{\mu^2} + \alpha_2 \frac{3}{2} \log\frac{M_W^2}{\mu^2} \right],
$$
$$
D^{(B \to Z)}_{q\bar{q}}(\mu) = \frac{1}{4\pi} 2 \log\frac{\hat{s}}{\mu^2} \left[\alpha_{\text{em}}(I^Z)^2 \log\frac{M_Z^2}{\mu^2} + \delta_{\lambda L} \alpha_2 \frac{1}{2} \log\frac{M_W^2}{\mu^2} \right]. \tag{21}
$$

The factor $H_{q\bar{q},Z}$ encodes the matching from the SM to SCET$_{EW}$. At the order we are working it is 1 plus pure-QCD terms. Here, we do not explicitly show the pure-QCD part of the running and the matching expressions, which were considered in previous papers, see Refs. [15,16]. The hard function for the Compton channel is related to Eq. (19) by crossing.

The leading electroweak corrections for the soft and jet functions are

$$
S_{q\bar{q},Z}(k, \mu_f) = e^{-4Q^2 S(\mu_s, \mu_f)} \delta(k);
$$
$$
J_q(p^2, \mu_f) = e^{-4Q^2 S(\mu_j, \mu_f)} \delta(p^2), \tag{22}
$$

and $S_{qg,Z}$ and J_g remain delta functions at this order. $S(\nu, \mu)$ in Eq. (22) is given by Eq. (11) with $\Gamma = \frac{\alpha_{\text{em}}}{4\pi}\Gamma_0$. As we will discuss in the next section, we will not include subleading electroweak corrections in the soft and jet functions for our numerical evaluations, therefore, we do not write them explicitly.

The results for direct photon production can readily be obtained from the ones for Z production given above. The hard function in the photon case can be obtained from the corresponding equation for the Z case, Eq. (19), with the following changes: (i) M_Z should be set to 0 inside the parenthesis in the first line and in $H_{q\bar{q},Z}(\hat{s}, \hat{t}, M_Z, \mu_h)$, (ii) the matching condition at μ_l should be changed according to the following substitution:

$$
c_W \sqrt{\alpha_2(\mu_h)} t^3 \mathcal{D}^{(W^3 \to Z)}_{q\bar{q}} \to s_W \sqrt{\alpha_2(\mu_h)} t^3 \mathcal{D}^{(W^3 \to \gamma)}_{q\bar{q}},
$$
$$
-s_W \sqrt{\alpha_1(\mu_h)} Y \mathcal{D}^{(B \to Z)}_{q\bar{q}} \to c_W \sqrt{\alpha_1(\mu_h)} Y \mathcal{D}^{(B \to \gamma)}_{q\bar{q}}, \tag{23}
$$

with $\mathcal{D}^{(W^3 \to \gamma)}_{q\bar{q}} = \mathcal{D}^{(W^3 \to Z)}_{q\bar{q}}$ and $\mathcal{D}^{(B \to \gamma)}_{q\bar{q}} = \mathcal{D}^{(B \to Z)}_{q\bar{q}}$ at the order we are working, and (iii) $\mathcal{U}^{(Z)}_{q\bar{q}}(\mu_l, \mu_f) \to \mathcal{U}^{(\gamma)}_{q\bar{q}}(\mu_l, \mu_f)$. At the order we need them, the anomalous dimensions for $\mathcal{U}^{(\gamma)}_{q\bar{q}}$ are given by

$$\Gamma^{(\gamma)} = \Gamma^{(Z)}, \qquad (24)$$

$$\gamma_{q\bar{q}}^{(\gamma)} = \gamma_{q\bar{q}}^{(Z)} - \frac{\alpha_{\text{em}}}{4\pi} \beta_0^{\alpha_{\text{em}}}. \qquad (25)$$

The electroweak corrections to the soft functions are the same as in the Z case, see Eq. (22). In principle there is now a jet function J_γ for the photon, which contains contributions from light fermions, analogous to the ones in the QCD jet function for the gluon. Those were not present in the Z case because there we had a HQET field. As we will discuss below in Sec. III B, we do not need to include these terms. The photon jet function is therefore just a delta function and we recover the same structure for the factorization formula that we had in the Z case.

B. Scale setting and numerical results

To evaluate the cross section numerically, we need to set the values of the different scales that appear in the SCET factorization formula, when both electroweak and Sudakov corrections are included. We recall that the electroweak corrections can be quite significant, around 20% for p_T around 1 TeV, but the pure-QCD corrections are, of course, also important. The hard, jet, and soft scales that are appropriate for the pure-QCD terms were determined in Refs. [15,16], following the procedure advocated in Ref. [10]. They were obtained as

$$\mu_h = \frac{13 p_T + 2 M_V}{12} - \frac{p_T^2}{\sqrt{s}};$$
$$\mu_j = \frac{7 p_T + 2 M_V}{12} \left(1 - 2\frac{p_T}{\sqrt{s}}\right), \qquad (26)$$

and $\mu_s = \mu_j^2/\mu_h$. The hard scale in Eq. (26) is of order p_T and therefore also adequate for the electroweak corrections. On the other hand, to resum the electroweak Sudakov corrections, we performed a running from μ_h to the low scale μ_l in the unbroken gauge theory, and then matched to a broken gauge theory. We use $\mu_l \sim M_V$, since this is the scale at which we integrate out the massive gauge bosons. The jet and soft functions are then defined below the scale μ_l and contain only light degrees of freedom, but no W or Z bosons, as is appropriate for the observable we are studying. The jet and soft scales in Eq. (26), though, are above M_V for values of p_T where the LHC will measure, and there is thus an apparent difficulty here, in the sense that the QCD values for the scales are not appropriate for the electroweak corrections. In practice, this does not lead to problems because the main part of the electroweak corrections is contained in the hard function: we have checked that the change in the cross section due to the leading electroweak corrections of the jet and soft functions is at the level of 1% or below for the range of p_T we study. Therefore, we can consider the jet and soft

functions just with leading electroweak corrections; at this order the strong and electroweak corrections do not mix [see Eq. (22)], and we can effectively set $\mu_j = M_V$ just in the electroweak part of the jet function. The alternative to that would be to choose μ_j and μ_s of order M_V everywhere, which would be in accordance with the chain of effective theories we used to resum the electroweak Sudakov corrections. There is not any obstacle to do that, but this scale setting would generate larger uncertainties in the QCD part, and the final result would be less precise. It is therefore better to ignore the subleading, numerically negligible, electroweak corrections in the jet and soft functions, and to use the scales in Eq. (26) everywhere except in the electroweak part of the jet and soft functions, where we use $\mu_j = M_V$, and $\mu_s = \mu_j^2/\mu_h$, accordingly.

Having set the scales, we now present plots of the results for the cross section for Z production. We include electroweak Sudakov as well as QCD corrections. The default values for the scales μ_h, μ_j, and μ_s are fixed according to the discussion above. The default values for the low-matching scale, μ_l, and the factorization scale, μ_f, are $\mu_l = \mu_f = M_V$. We will vary these scales by a factor of 2 to estimate the uncertainties. In all our plots we use the next-to-next-to-leading order MSTW 2008 PDF set [51]. Note that for consistency of the factorization formula one should include quantum electrodynamics (QED) effects in the PDFs. This PDF set, though, does not include QED effects. There are some older PDF sets that do include QED corrections [52], but these have lower accuracy for the QCD part. Since the QED corrections in the PDFs should not be very important according to our discussion above, it is better to use a newer PDF set with higher QCD orders. The numerical values for the couplings and masses that we use read $M_Z = 91.1876$ GeV, $M_W = 80.399$ GeV, $\alpha_s(M_Z) = 0.1171$, $\alpha_{\text{em}}(M_Z) = (127.916)^{-1}$, $\sin^2\theta_W = 0.2226$, $V_{ud} = 0.97425$, $V_{us} = 0.22543$, $V_{ub} = 0.00354$, $V_{cd} = 0.22529$, $V_{cs} = 0.97342$ and $V_{cb} = 0.04128$. We present our results for the LHC at 7 TeV, for an easier comparison with the results in Ref. [16]. The relative size of the corrections is very similar at 13 TeV.

To show the effect of including electroweak corrections to the cross section, we plot in Fig. 2 the difference

$$\Delta\sigma^{\text{ew}} := \frac{\sigma_{\text{ew}}^i - \sigma^i}{\sigma^i}, \qquad (27)$$

where σ^i represents the cross section with QCD corrections at order N^{i}LL, while σ_{ew}^i also includes the electroweak corrections. The electroweak corrections are always included at the same order, independently of the value of i; i.e. including terms up to order a in the exponent for the hard function, and the leading corrections in the jet and soft functions. In the figure, the black curves and bands correspond to $i = 1$, and the green ones
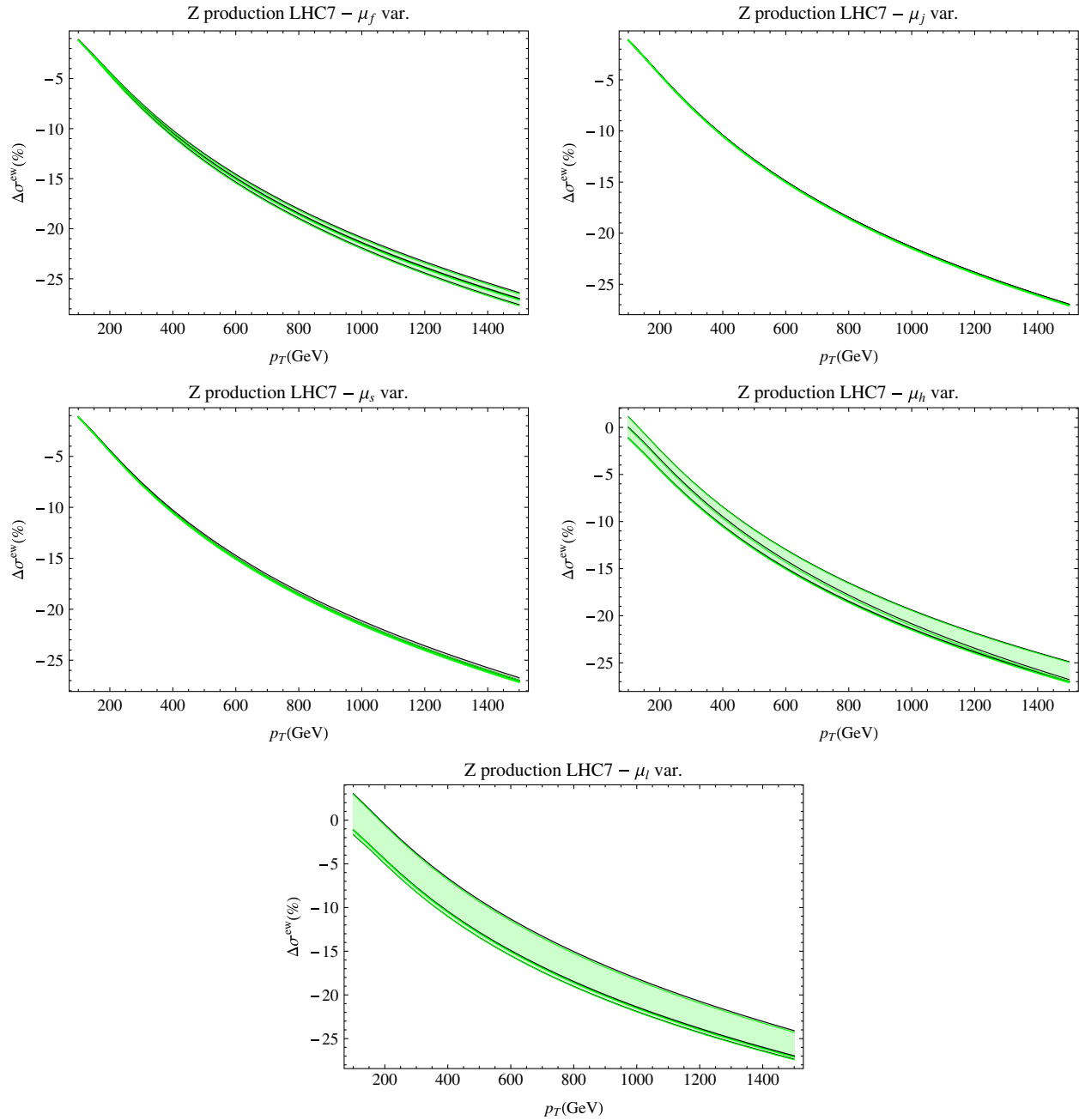
FIG. 2 (color online). *Z* production for the LHC at 7 TeV. We plot the difference of cross sections with and without electroweak corrections, normalized to the QCD result, as defined in Eq. (27). The black (darker) curves and bands correspond to $i = 1$, and the green (lighter) ones to $i = 2$, note that they basically overlap. In each plot we vary the corresponding scale, denoted at the top, by a factor of 2.

to $i = 2$. Again, in each plot we have varied the corresponding scale by a factor of 2. The scales in the QCD and the electroweak parts are varied simultaneously, both in the numerator and denominator of Eq. (27). From the fact that the black and green curves are almost identical, we learn that in order to study the relative importance of the electroweak corrections it is not necessary to include the QCD corrections at N²LL accuracy. To better visualize the effect of the scale variations,

we choose a reference value $p_T = 500$ GeV and plot the cross section as a function of the deviation from the default scale choices; this is shown in Fig. 3, for both the *Z* boson and the photon. We observe that the electroweak corrections in the cross section for photon production are smaller than those for *Z* production. For our final results, which are shown in Fig. 5, we add the bands coming from the different scale variations in quadrature.
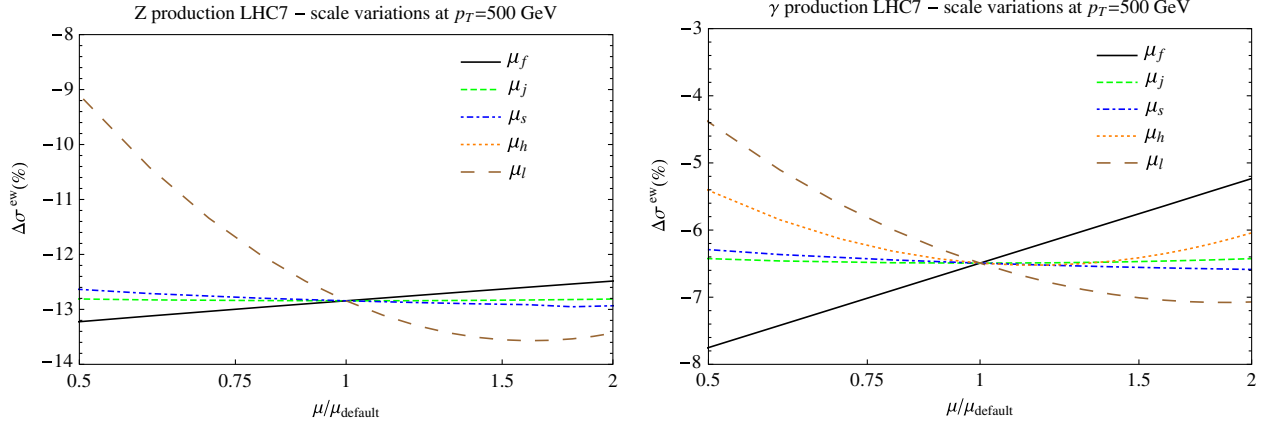
FIG. 3 (color online).   Effect of scale variations in the cross section for Z and γ production at $p_T = 500$ GeV as a reference point.

IV. RESULTS FOR W PRODUCTION

We now consider single W-boson production. The main difference with respect to Z production is that the $W^\pm$ bosons are charged. Therefore, both particles in the final state, the $W^\pm$ and the quark or gluon, can have a jet function. This means that the factorization formula is more complicated than in the previous section, and will have the general form sketched in Eq. (1). The situation is similar to the study of QCD corrections to dijet cross sections. A factorization formula for those processes was derived in Ref. [53], and the ingredients for N^{2}LL resummation in SCET were given in Refs. [54,55]. The expression that we will use here has the same form as the one in Ref. [55], but is simpler, because we only have one possible group structure (the tree level diagrams contain one $SU(3)_C$ and one $SU(2)_L$ matrix, but those are in different spaces and commute), in contrast to the dijet case. Therefore, the H and S functions in the factorization formula have no group indices. We write the partonic cross section for the channel $ab \to cW$ as

$$\hat{s}\frac{d\hat{\sigma}_{ab,W}}{d\hat{s}d\hat{t}} = \hat{\sigma}^B_{ab,W} H_{ab,W}(\hat{s},\hat{t},M_W,\mu)$$
$$\times \int dp_W^2 dp_c^2 dk J_W(p_W^2,\mu) J_c(p_c^2,\mu) S_{ab,W}(k,\mu)$$
$$\times \delta(M_X^2 + M_W^2 - p_W^2 - p_c^2 - 2E_J k), \quad (28)$$

and the hadronic cross section is then obtained after performing the convolution with the PDFs, analogous to Eq. (16). Since we will only include electroweak corrections to the jet and soft functions at leading order, J_W reduces to a $\delta(p_W^2 - M_W^2)$ times a prefactor, and we recover the structure for the factorization formula that we had in the Z case. In the following we give the results for the different ingredients of the factorization formula above.

The $W^\pm$ bosons in the broken theory come from the $SU(2)_L$ gauge bosons $W^{1,2}$ in the unbroken theory, according to the combination $W^\pm = 1/\sqrt{2}(W^1 \mp iW^2)$. Amplitudes with a W^1 or a W^2 receive the same electroweak corrections as those for W^3 in the previous section, i.e. the evolution factor $\mathcal{U}^{(W^3)}_{ab}(\mu_h,\mu_l)$ in Eq. (19). Below the scale μ_l, the $W^\pm$ boson is treated as a field in HQET. The low-energy matching is given by[1]

$$D^{(W^\pm \to W^\pm)}_{q\bar{q}}(\mu)$$
$$= D^{(W^3 \to Z)}_{q\bar{q}}(\mu) + \frac{\alpha_2}{4\pi}\log\frac{\hat{s}}{\mu^2}\left[-\log\frac{M_W^2}{\mu^2} + c_W^2\log\frac{M_Z^2}{\mu^2}\right], \quad (29)$$

and the running in the low-energy broken theory is given by the corresponding factor, $\mathcal{U}^{(W^\pm)}_{q\bar{q}}(\mu_l,\mu_f)$, with the following anomalous dimensions:

$$\Gamma^{(W^\pm)} = \frac{\alpha_{em}}{4\pi}\frac{\Gamma_0}{2}(Q^2 + Q'^2), \quad (30)$$

$$\gamma^{(W^\pm)}_{q\bar{q}} = \frac{\alpha_{em}}{4\pi}\left[-\Gamma_0\frac{1}{2}\log\frac{M_W^2}{\hat{s}} - \Gamma_0 QQ' i\pi \right.$$
$$+ \Gamma_0 Q Q_{W^\pm}\log\frac{-\hat{t}}{\hat{s}} - \Gamma_0 Q' Q_{W^\pm}\log\frac{-\hat{u}}{\hat{s}}$$
$$\left. - 3(Q^2 + Q'^2) - 2\right], \quad (31)$$

where Q is the charge of the quark and $-Q'$ the charge of the antiquark (i.e. $Q - Q' = Q_{W^\pm}$, with $Q_{W^\pm}$ the charge of the $W^\pm$ boson). Since the $W^\pm$ is massive in the low-energy theory, the expression Eq. (4) cannot be used to obtain the above anomalous dimension. The appropriate expression for the massive case was given in [56]. The hard function times Born-level cross section is then given by

---

[1] For simplicity, we use the subscript $q\bar{q}$ in $D^{(W^\pm \to W^\pm)}_{q\bar{q}}$, despite the fact that the two quarks have different flavor.
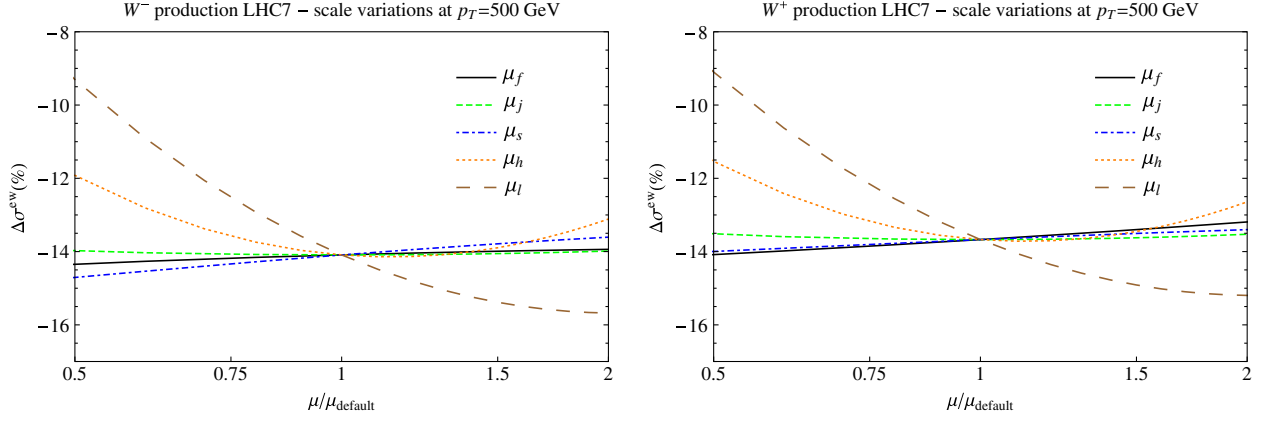
FIG. 4 (color online). Effect of scale variations in the cross section for W^- and W^+ production at $p_T = 500$ GeV as a reference point.
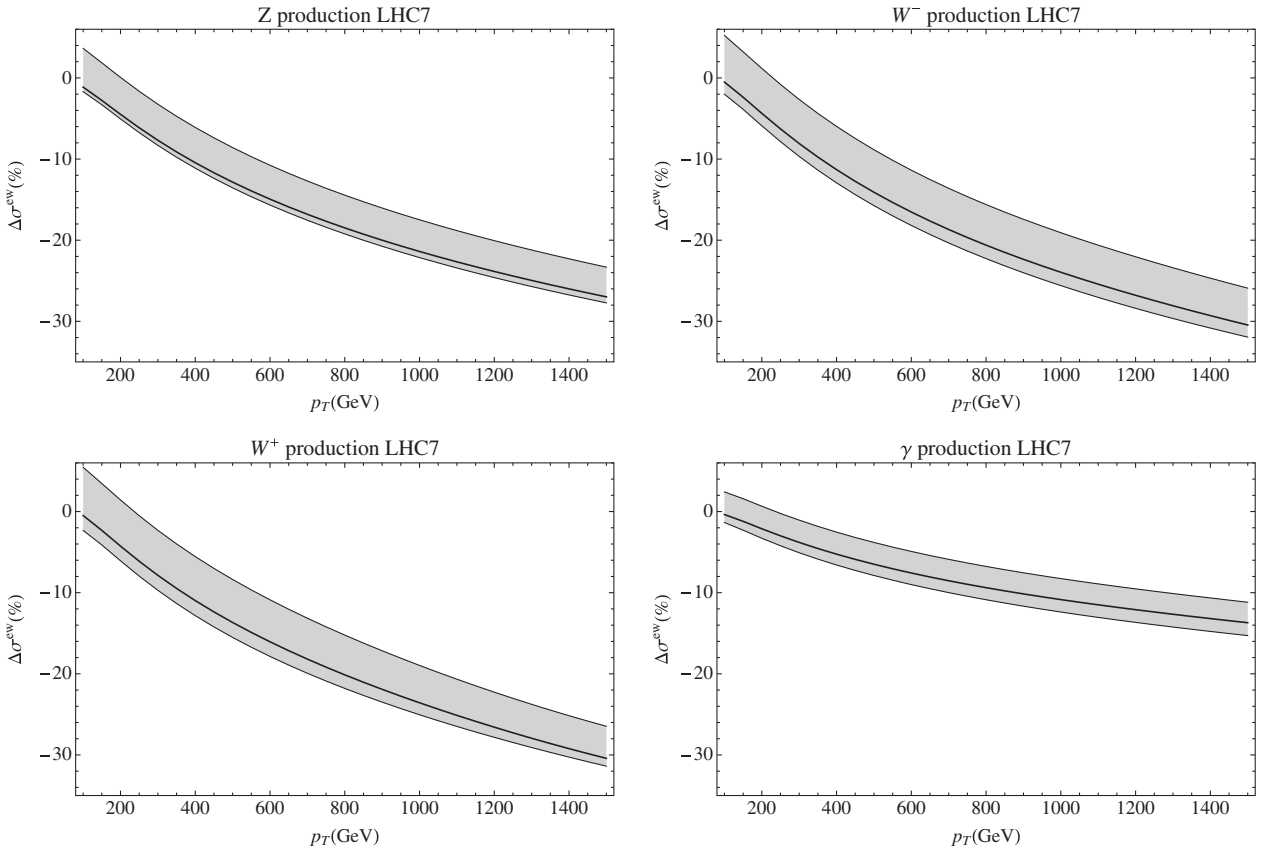

FIG. 5. W, Z and γ production for the LHC 7 TeV. We plot the difference of cross sections with and without electroweak corrections given by Eq. (27), with $i = 1$. The bands reflect the perturbative uncertainty of the results. They are obtained by first varying each of the scales appearing in the factorization formula by a factor of 2 (as discussed in the text), and then adding these different individual bands in quadrature.

$$\hat{\sigma}^B_{q\bar{q},W^\pm} H_{q\bar{q},W^\pm}(\hat{s}, \hat{t}, M_W, \mu_f) = \frac{\pi \alpha_s(\mu_h)}{\hat{s}} \frac{2C_F}{N_c} \left(\frac{\hat{t}^2 + \hat{u}^2 + 2M_W^2 \hat{s}}{\hat{t}\,\hat{u}} \right) \left| \mathcal{U}^{(W^\pm)}_{q\bar{q}}(\mu_l, \mu_f) \right|^2$$

$$\times \left| \frac{V_{ij}}{\sqrt{2}} \sqrt{\alpha_2(\mu_h)} \mathcal{D}^{(W^\pm \to W^\pm)}_{q\bar{q}}(\mu_l) \mathcal{U}^{(W^\pm)}_{q\bar{q}}(\mu_h, \mu_l) \right|^2 H_{q\bar{q},W^\pm}(\hat{s}, \hat{t}, M_W, \mu_h). \qquad (32)$$

Here, V_{ij} denotes the Cabibbo-Kobayashi-Maskawa matrix and we have assumed that the quark and antiquark are from generations i and j, respectively. Like in the Z case of the previous section, we do not write pure-QCD corrections explicitly, and $H_{ab,W}(\hat{s}, \hat{t}, M_W, \mu_h)$ is again 1 plus pure-QCD terms at the order we are working. The expression for the Compton channel can be obtained from the result in Eq. (32) above by crossing.

The $W^\pm$ jet function is defined in HQET, see Ref. [57]. At the order we need here we have

$$J_W(p^2, \mu_f) = e^{-4S(\mu_j, \mu_f)}\delta(p^2 - M_W^2), \qquad (33)$$

with $S(\nu, \mu)$ given by Eq. (11) with $\Gamma = \frac{\alpha_{em}}{2\pi}$. Finally, for the leading electroweak corrections to the soft functions that we need in this case we obtain

$$
\begin{aligned}
S_{q\bar{q},W}(k, \mu_f) &= e^{-4(Q^2 + Q'^2 - 1)S(\mu_s, \mu_f)}\delta(k); \\
S_{qg,W}(k, \mu_f) &= e^{-4(Q^2 - Q'^2 - 1)S(\mu_s, \mu_f)}\delta(k),
\end{aligned} \qquad (34)
$$

again with $S(\nu, \mu)$ given by Eq. (11) with $\Gamma = \frac{\alpha_{em}}{2\pi}$.

We show the effect of the different scale variations for $W^\pm$ production in Fig. 4. The final results for the cross section are shown in Fig. 5. The results for $W^\pm$ are numerically quite similar to the Z-boson case.

V. SUMMARY AND CONCLUSIONS

In summary, in this paper we have computed electroweak Sudakov corrections to the cross sections for single W, Z and γ production at large transverse momentum, within SCET using the approach of Refs. [36,37]. We have presented complete results for the factorized hadronic cross sections with electroweak corrections. At the LHC, these corrections are of order 20% for $p_T \sim 1$ TeV for Z and W production and about half as big for prompt photon production. Their inclusion is necessary to obtain precise predictions of the spectrum at large p_T. In our numerical analysis, we included both QCD and electroweak corrections, and discussed the most adequate way to set the different scales that appear in the factorized form for the cross section. Our results are summarized in Fig. 5, where we show the effect of including electroweak corrections in the cross section by plotting the difference of cross sections with and without electroweak corrections.

Two important features of our results are the following: first of all, the main part of the electroweak corrections is contained in the hard function, and the effects on the jet and soft functions are much smaller. This is also evident from the fact that the bands due to μ_j and μ_s variation in Fig. 2 are much smaller than the ones coming from the variation of the other scales. This result is in accordance with the statements made in Ref. [30]

regarding the small impact of the different treatments of singularities in real radiation photon diagrams on the size of the corrections [29,30]. The second feature worth stressing is that the relative importance of the electroweak corrections, as defined in Eq. (27), does not depend much on the order to which we work in the QCD part. This means that one can, to good accuracy, include electroweak effects via an overall prefactor in existing pure-QCD computations.

Electroweak Sudakov corrections to vector-boson production have been considered before. In particular, Refs. [25,27,30] have presented analytic expressions for the IR-finite part of the virtual electroweak corrections, at next-to-leading logarithmic accuracy up to two loops, in the limit $M_{W,Z}^2 \ll \hat{s} \sim \hat{t} \sim \hat{u}$, for Z, γ and $W^\pm$ production, respectively. These terms correspond to our expressions for $\hat{\sigma}_{q\bar{q},V}^B H_{q\bar{q},V}$ expanded to order α_i^3, with $\mu_l = \mu_f = M_W = M_Z$. References [25,27,30] do not consider QCD corrections and the mixing terms $S_{\alpha_s \alpha_i}(\nu, \mu)$ are therefore not included in their results. Switching off the QCD terms in our result and performing a fixed-order expansion, we find agreement with their results.

The results of this paper together with the resummation of the pure-QCD corrections, which can be performed at N^3LL accuracy, yield predictions for single electroweak-boson production at large transverse momentum at an unprecedented level of accuracy. Ratios of these p_T spectra can be used to constrain the u/d ratio of PDFs or as a theoretical input in estimations of the $Z(\rightarrow \nu\bar{\nu})+$ jets background to new physics searches, as recently discussed in Ref. [58]. A comprehensive study comparing with available LHC data, including N^3LL accuracy for the pure-QCD resummation, will be the subject of a future publication.

APPENDIX: BETA FUNCTIONS IN THE SM

The two-loop running of a general direct-product group can be found in Ref. [59]. Recently, the running of the couplings in the SM up to three loops has also been computed, in Refs. [60–62]. For convenience this Appendix collects the expressions for the SM beta functions that are used throughout the paper.

We write the beta function for the coupling α_a as

$$
\begin{aligned}
\beta(\alpha_a) = -2\alpha_a\bigg[&\beta_0^{\alpha_a}\frac{\alpha_a}{4\pi} + \beta_1^{\alpha_a}\Big(\frac{\alpha_a}{4\pi}\Big)^2 \\
&+ \beta_1^{\alpha_a\alpha_b}\frac{\alpha_a}{4\pi}\frac{\alpha_b}{4\pi} + \cdots \bigg].
\end{aligned} \qquad (A1)
$$

The coefficients that are used in the paper read

$$\beta_0^{\alpha_1} = \frac{5}{3}\left(-\frac{4}{3}n_g - \frac{1}{10}n_h\right) = -\frac{41}{6},$$

$$\beta_0^{\alpha_2} = \frac{22}{3} - \frac{4}{3}n_g - \frac{1}{6}n_h = \frac{19}{6},$$

$$\beta_1^{\alpha_s\alpha_1} = -\frac{5}{3}\frac{11n_g}{30} = -\frac{11}{6},$$

$$\beta_1^{\alpha_s\alpha_2} = -\frac{3n_g}{2} = -\frac{9}{2},$$

$$\beta_1^{\alpha_1\alpha_s} = -\frac{5}{3}\frac{44n_g}{15} = -\frac{44}{3},$$

$$\beta_1^{\alpha_2\alpha_s} = -4n_g = -12,$$

$$\beta_0^{\alpha_{em}} = -\frac{4}{3}[N_c(3Q_d^2 + 2Q_u^2) + 3Q_l^2] = -\frac{80}{9},$$

$$\beta_1^{\alpha_s\alpha_{em}} = 2(3Q_d^2 + 2Q_u^2) = -\frac{22}{9},$$

$$\beta_1^{\alpha_{em}\alpha_s} = -4C_F[N_c(3Q_d^2 + 2Q_u^2)] = -\frac{176}{9},$$

(A2)

where $n_g = 3$ is the number of generations, $n_h = 1$ is the number of Higgs doublets, $C_F = (N_c^2 - 1)/(2N_c)$, $N_c = 3$ is the number of colors, $Q_d = -1/3$ and $Q_u = 2/3$ are the charges of the down- and up-type quarks respectively, and $Q_l = -1$ is the charge of the charged leptons.

---

[1] R. K. Ellis, G. Martinelli, and R. Petronzio, Nucl. Phys. **B211**, 106 (1983).
[2] P. B. Arnold and M. H. Reno, Nucl. Phys. **B319**, 37 (1989).
[3] R. J. Gonsalves, J. Pawlowski, and C.-F. Wai, Phys. Rev. D **40**, 2245 (1989).
[4] J. Campbell, K. Ellis, and C. Williams, http://mcfm.fnal.gov/.
[5] R. Gonsalves, http://www.physics.buffalo.edu/gonsalves/ewbqt/index.html.
[6] K. Melnikov and F. Petriello, Phys. Rev. D **74**, 114017 (2006).
[7] S. Catani, L. Cieri, G. Ferrera, D. de Florian, and M. Grazzini, Phys. Rev. Lett. **103**, 082001 (2009).
[8] R. Gavin, Y. Li, F. Petriello, and S. Quackenbush, Comput. Phys. Commun. **182**, 2388 (2011).
[9] E. Laenen, G. Oderda, and G. F. Sterman, Phys. Lett. B **438**, 173 (1998).
[10] T. Becher, M. Neubert, and G. Xu, J. High Energy Phys. 07 (2008) 030.
[11] C. W. Bauer, S. Fleming, D. Pirjol, and I. W. Stewart, Phys. Rev. D **63**, 114020 (2001).
[12] C. W. Bauer, D. Pirjol, and I. W. Stewart, Phys. Rev. D **65**, 054022 (2002).
[13] M. Beneke, A. P. Chapovsky, M. Diehl, and T. Feldmann, Nucl. Phys. **B643**, 431 (2002).
[14] T. Becher and M. D. Schwartz, J. High Energy Phys. 02 (2010) 040.
[15] T. Becher, C. Lorentzen, and M. D. Schwartz, Phys. Rev. Lett. **108**, 012001 (2012).
[16] T. Becher, C. Lorentzen, and M. D. Schwartz, Phys. Rev. D **86**, 054026 (2012).
[17] N. Kidonakis and R. J. Gonsalves, Phys. Rev. D **87**, 014001 (2013).
[18] L. W. Garland, T. Gehrmann, E. W. N. Glover, A. Koukoutsakis, and E. Remiddi, Nucl. Phys. **B627**, 107 (2002).
[19] L. W. Garland, T. Gehrmann, E. W. N. Glover, A. Koukoutsakis, and E. Remiddi, Nucl. Phys. **B642**, 227 (2002).
[20] T. Gehrmann and E. Remiddi, Nucl. Phys. **B640**, 379 (2002).
[21] T. Gehrmann and L. Tancredi, J. High Energy Phys. 02 (2012) 004.
[22] T. Becher and G. Bell, Phys. Lett. B **695**, 252 (2011).
[23] T. Becher and M. Neubert, Phys. Lett. B **637**, 251 (2006).
[24] T. Becher, G. Bell, and S. Marti, J. High Energy Phys. 04 (2012) 034.
[25] J. H. Kuhn, A. Kulesza, S. Pozzorini, and M. Schulze, Phys. Lett. B **609**, 277 (2005).
[26] J. H. Kuhn, A. Kulesza, S. Pozzorini, and M. Schulze, Nucl. Phys. **B727**, 368 (2005).
[27] J. H. Kuhn, A. Kulesza, S. Pozzorini, and M. Schulze, J. High Energy Phys. 03 (2006) 059.
[28] J. H. Kuhn, A. Kulesza, S. Pozzorini, and M. Schulze, Phys. Lett. B **651**, 160 (2007).
[29] W. Hollik, T. Kasprzik, and B. A. Kniehl, Nucl. Phys. **B790**, 138 (2008).
[30] J. H. Kuhn, A. Kulesza, S. Pozzorini, and M. Schulze, Nucl. Phys. **B797**, 27 (2008).
[31] M. Ciafaloni, P. Ciafaloni, and D. Comelli, Phys. Rev. Lett. **84**, 4810 (2000).
[32] W. J. Stirling and E. Vryonidou, J. High Energy Phys. 04 (2013) 155.
[33] J.-y. Chiu, F. Golf, R. Kelley, and A. V. Manohar, Phys. Rev. Lett. **100**, 021802 (2008).
[34] J.-y. Chiu, F. Golf, R. Kelley, and A. V. Manohar, Phys. Rev. D **77**, 053004 (2008).
[35] J.-y. Chiu, R. Kelley, and A. V. Manohar, Phys. Rev. D **78**, 073006 (2008).
[36] J.-y. Chiu, A. Fuhrer, R. Kelley, and A. V. Manohar, Phys. Rev. D **80**, 094013 (2009).
[37] J.-y. Chiu, A. Fuhrer, R. Kelley, and A. V. Manohar, Phys. Rev. D **81**, 014023 (2010).
[38] A. Denner, S. Dittmaier, T. Kasprzik, and A. Muck, J. High Energy Phys. 08 (2009) 075.
[39] A. Denner, S. Dittmaier, T. Kasprzik, and A. Muck, J. High Energy Phys. 06 (2011) 069.

[40] T. Becher and M. Neubert, Phys. Rev. Lett. **102**, 162001 (2009).

[41] T. Becher and M. Neubert, J. High Energy Phys. 06 (2009) 081.

[42] E. Gardi and L. Magnea, J. High Energy Phys. 03 (2009) 079.

[43] L. J. Dixon, E. Gardi, and L. Magnea, J. High Energy Phys. 02 (2010) 081.

[44] V. Del Duca, C. Duhr, E. Gardi, L. Magnea, and C. D. White, J. High Energy Phys. 12 (2011) 021.

[45] V. Ahrens, M. Neubert, and L. Vernazza, J. High Energy Phys. 09 (2012) 138.

[46] T. Becher, M. Neubert, and B. D. Pecjak, J. High Energy Phys. 01 (2007) 076.

[47] V. A. Smirnov, Phys. Lett. B **404**, 101 (1997).

[48] T. Becher and M. Neubert, Eur. Phys. J. C **71**, 1665 (2011).

[49] J.-Y. Chiu, A. Jain, D. Neill, and I. Z. Rothstein, J. High Energy Phys. 05 (2012) 084.

[50] S. Fleming, A. H. Hoang, S. Mantry, and I. W. Stewart, Phys. Rev. D **77**, 074010 (2008).

[51] A. D. Martin, W. J. Stirling, R. S. Thorne, and G. Watt, Eur. Phys. J. C **63**, 189 (2009).

[52] A. D. Martin, R. G. Roberts, W. J. Stirling, and R. S. Thorne, Eur. Phys. J. C **39**, 155 (2005).

[53] N. Kidonakis, G. Oderda, and G. F. Sterman, Nucl. Phys. **B525**, 299 (1998).

[54] R. Kelley and M. D. Schwartz, Phys. Rev. D **83**, 045022 (2011).

[55] R. Kelley and M. D. Schwartz, Phys. Rev. D **83**, 033001 (2011).

[56] T. Becher and M. Neubert, Phys. Rev. D **79**, 125004 (2009); **80**, 109901(E) (2009).

[57] S. Fleming, A. H. Hoang, S. Mantry, and I. W. Stewart, Phys. Rev. D **77**, 114003 (2008).

[58] S. A. Malik and G. Watt, arXiv:1304.2424.

[59] D. R. T. Jones, Phys. Rev. D **25**, 581 (1982).

[60] L. N. Mihaila, J. Salomon, and M. Steinhauser, Phys. Rev. Lett. **108**, 151602 (2012).

[61] L. N. Mihaila, J. Salomon, and M. Steinhauser, Phys. Rev. D **86**, 096008 (2012).

[62] A. V. Bednyakov, A. F. Pikelner, and V. N. Velizhanin, J. High Energy Phys. 01 (2013) 017.